

# RKKY interaction and two Kondo impurities: the complete phase diagram

Krzysztof P. Wójcik<sup>1,2,\*</sup> and Johann Kroha<sup>1,†</sup>

<sup>1</sup>*Physikalisches Institut, Universität Bonn, Nussallee 12, D-53115 Bonn, Germany*

<sup>2</sup>*Institute of Molecular Physics, Polish Academy of Sciences, Smoluchowskiego 17, 60-179 Poznań, Poland*

(Dated: June 15, 2021)

Since Jones-Varma seminal works the indirect RKKY interaction is usually modeled as independently tunable Heisenberg spin exchange. For such a model in particle-hole-symmetric case there is always a quantum phase transition between Kondo and RKKY phases, even in the resonant regime (*i.e.* when impurity-host coupling exceeds Coulomb interaction strength). We show, that for the simple model with RKKY interaction genuinely induced by Kondo couplings and the inter-host interaction, either two phase transitions occur or none, depending on the Kondo coupling strength. Each transition corresponds to destruction of effective quasi-particles by the relevant spin exchange and occurs at spin exchange strength of the order of the quasi-particle bandwidth. Similar results are expected for all quantum phase transitions induced by indirect interactions. Furthermore, we confirm earlier perturbative prediction of the Kondo breakdown at a finite Kondo temperature,  $T_K = T_K^0/e$ , with  $T_K$  meaning the scale where departure from high-energy local-moment regime happens, while strong-coupling or RKKY fixed points are achieved at arbitrarily small energy scales close to the transition. These findings may be relevant for heavy-fermion materials via DMFT mapping. We also propose experimental setup with 2-impurity system involving flat-band Moiré material for direct test of our predictions.

*Introduction.*—Understanding and utilization of exotic properties of different materials lies in the heart of physics of strong correlations. Often the unusual properties stem from the competition between two quite conventional phases, which can be described in terms of free effective quasi-particles. When the interaction between the latter overcomes their natural energy scale, the relevant quasi-particles change abruptly at a critical strength of the interaction, which is seen as a quantum phase transition (QPT). In the vicinity of such a critical point, the system may exhibit non-Fermi-liquid behavior [1–4].

A prominent example of such a scenario is the Jones-Varma (JV) QPT in two-impurity systems [5–7]. For a single impurity coupled to a metallic host the ground state is always the Kondo singlet, and the elementary excitations form a Fermi liquid characterized by a single energy scale called the Kondo temperature,  $T_K$ , which plays a role of their band-width [8]. However, a Heisenberg-type spin exchange coupling the two impurities,  $J_H$ , destabilizes the Kondo quasi-particles at the critical strength  $J_H^*$  of the order of  $T_K$ , and the conduction-band Bloch electrons take over the role of effective quasi-particles.

The JV example is of inappreciable importance, as it has been conjectured that a similar scenario (named after Doniach) is realized in dense lattices of impurities [1, 2, 9], where the indirect Ruderman-Kittel-Kasuya-Yosida (RKKY) interaction  $Y$  [10–12] provides the inter-impurity exchange. The controlled solution of the lattice model is so far not available, which leaves a lot of space for speculations concerning the validity of Doniach picture. However, not only has it been challenged by the Nozieres’ exhaustion proposal [13, 14] and existence of other screening mechanisms [15] in the lattice context, but already relevance of the results of Refs. [5–7]

to the case of two impurities sharing the common host has experienced a lot of critics. In particular, the QPT is fragile to particle-hole (PH) asymmetry, which changes the QPT into a crossover [16, 17]. This has led to the widespread belief that QPT is not present in a realistic 2-impurity system and has made its relevance for lattice models debatable. Moreover, it has even been shown that the anti-ferromagnetic contribution to  $Y$  stems from the PH-asymmetric component of the effective Hamiltonian, so the QPT is in general absent in properly modeled two-impurity system with a single host [17–19]. Yet, for weaker PH symmetry conditions the QPT can be restored by single-parameter fine-tuning, since there is only one asymmetry-related operator which is marginally relevant around the QPT fixed point [19]. Moreover, QPT has been seen in an experiment on a properly tailored two-impurity system, where each impurity is coupled to a different host [20]. As we show further, QPT is also present for the PH-symmetric hosts coupled only by spin exchange, which does not introduce charge transfer. Therefore, one can conclude QPT is indeed relevant for properly tailored systems at least in the case of two impurities, and its good understanding seems indispensable for properly pinpointing the lattice scenarios.

Less stressed in the literature is another flaw of the JV treatment of two-impurity model, namely that in Refs. [5–7]  $Y$  and the Kondo exchange (denoted here  $J_K$ ) are considered independent, although  $Y$  is genuinely generated from  $J_K$ , and the Kondo temperature depends on  $Y$ , as has been shown experimentally [20] and theoretically [21]. We revisit the problem to show, by numerical renormalization group (NRG) calculations [22–24], that in the geometry of two impurities coupled each to a different host as in Ref. [20],  $Y$  induced solely by  $J_K$  and the inter-host spin-exchange coupling  $J_Y$  causes the QPT

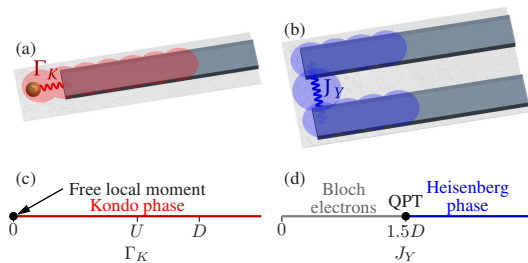


Figure 1. Illustration of the cloud of (a) Kondo quasi-particles and (b) Heisenberg quasi-particles, with corresponding phase diagrams (c) and (d).

for a properly symmetric case (hence, potentially for the fine-tuned weakly PH-symmetric case as well). Nevertheless, the most important observation is that  $J_Y$  also comes into play itself, and significantly alter the QPTs landscape. We show that apart from inducing  $Y$  and the JV QPT,  $J_Y$  leads to another QPT, at energy scale of the Bloch electrons band-width  $D$ , and may even lead to the suppression of the JV QPT for sufficiently strong  $J_K$ . We believe these possibilities to be generic for other QPTs triggered by indirect interactions, and propose a system where we hope it might be possible to observe this kind of behavior experimentally.

*Kondo and Heisenberg quasi-particles.*—Single-channel spin 1/2 Kondo model is well understood [8, 22, 25], as is its more general variant due to Anderson. Local coupling  $\Gamma_K$  between the impurity and the conduction band induces local spin exchange  $J_K$  and leads to the Kondo effect, *i.e.* a screening of the impurity moment through the bound-state formation at sufficiently low temperatures,  $T < T_K^0$ . This happens for any  $J_K > 0$ , due to the fact that  $J_K$  is subjected to the renormalization group flow toward the strong coupling fixed point [22], see phase diagram in Fig. 1(c). The ground state is a Fermi Liquid, and the effective quasi-particles form so-called Kondo cloud, which comprises of impurity and some of the conduction band degrees of freedom, as illustrated in Fig. 1(a). Despite the local character of both the impurity and its interaction with the host, the size of the cloud is not reduced to one site of the host, but is in fact a many-body object [26–29]. Normalized local spectral density at the impurity,  $\mathcal{A}(\omega) = -\Gamma_K \sum_{\sigma} \text{Im} \langle \langle d_{\sigma}, d_{\sigma}^{\dagger} \rangle \rangle^{\text{ret}}(\omega)$  (where  $d_{\sigma}$  annihilates a spin- $\sigma$  electron at the impurity), exhibits the Abrikosov-Suhl peak of height 1 and width  $\sim T_K^0$ , which is an effective bandwidth of the free Kondo quasi-particles. Meanwhile, the normalized spectral density of conduction band electrons at the impurity site,  $\mathcal{B}(\omega) = -2D \sum_{\sigma} \text{Im} \langle \langle c_{\sigma}, c_{\sigma}^{\dagger} \rangle \rangle^{\text{ret}}(\omega)$ , vanishes at low energies with a characteristic Fermi-liquid  $\mathcal{B}(\omega) \sim \omega^2$  dependence.

A similar phase appears when the impurity is substituted by a second metallic lead, *i.e.* for two metallic electrodes (without impurities), coupled by local exchange

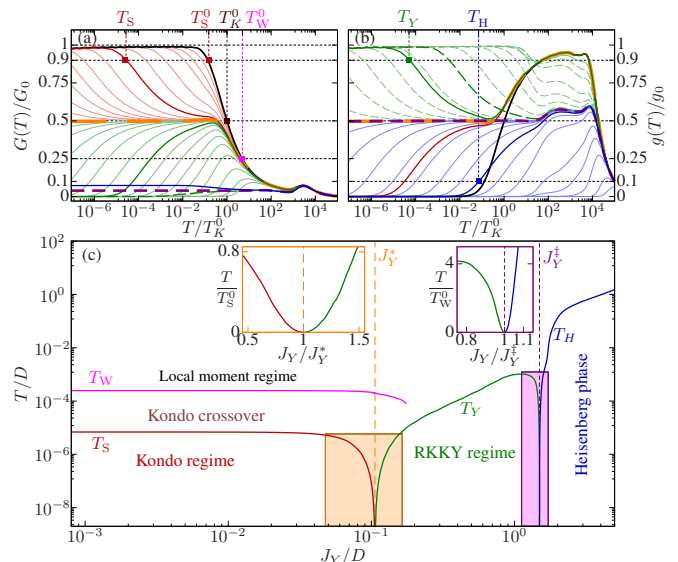


Figure 2. Crossover scales relevant for both transitions. (a) and (b) show temperature-broadened spectral densities at the relevant impurity and conduction band sites, respectively. Long (short) dashed lines were obtained for  $J_Y = J_Y^*$  ( $J_Y = J_Y^{\ddagger}$ ), correspondingly. Different energy scales can be recognized, as indicated, and their  $J_Y$  dependence is shown in (c). Insets in (c) zoom shaded areas around QPTs.

interaction  $J_Y$ . The Hamiltonian of such system can be then written as

$$H_{\text{leads}} = \sum_{\alpha \mathbf{k} \sigma} \varepsilon_{\alpha \mathbf{k}} c_{\alpha \mathbf{k} \sigma}^{\dagger} c_{\alpha \mathbf{k} \sigma} + J_Y \vec{s}_1 \circ \vec{s}_2, \quad (1)$$

where  $\alpha = 1$  or  $\alpha = 2$  label the leads,  $\varepsilon_{\alpha \mathbf{k}}$  is the dispersion relation for lead  $\alpha$ ,  $c_{\alpha \mathbf{k} \sigma}$  annihilates spin- $\sigma$  electron of momentum  $\mathbf{k}$  there, and local spin operators  $\vec{s}_i$  can be expressed in terms of Pauli matrices  $\vec{\tau}$  as  $\vec{s}_{\alpha} = \sum_{\mathbf{k} \mathbf{k}' \sigma \sigma'} v_{\alpha \mathbf{k}} v_{\alpha \mathbf{k}'}^* c_{\alpha \mathbf{k} \sigma}^{\dagger} \vec{\tau}_{\sigma \sigma'} c_{\alpha \mathbf{k}' \sigma'}/2$ . The inter-lead exchange coupling  $J_Y$  leads to the destruction of free band-electrons and formation of another Fermi liquid, however, unlike in the Kondo case, the coupling strength must exceed a critical value  $J_Y^{\ddagger}$  for this to happen. Our NRG calculations<sup>1</sup> show that  $J_Y^{\ddagger} \approx 1.5D$  in the case

<sup>1</sup> We use full density matrix approach to NRG [30], where the complete basis is constructed from states discarded during NRG iteration [31]. We use open-access code [24] as a basis for our programs.  $G(T)$  and  $g(T)$  are computed directly from discrete set of Dirac delta peaks, corresponding to  $T \rightarrow 0$  spectral function [32]. This allows for avoiding of artificial broadening. For data presented in Fig. 1(d), Fig. 2, and Fig. 3 we have taken discretization parameter  $\Lambda = 2.5$  and in each iteration we keep states with rescaled energy below a threshold  $E_{\text{cut}}$ , taken in the range [6.5, 7]. For Fig. 4 we have used  $\Lambda = 3$  and  $E_{\text{cut}} \in [4.5, 5]$ . The calculations are fastened by exploiting SU(2) or U(1) spin symmetry (reduced spin symmetry appears for susceptibilities calculations, where we have used staggered magnetic field of the order of  $100T$  to calculate a linear response) and two SU(2) charge symmetries (one per each host-impurity pair).

of metallic leads with identical, rectangular normalized density of states within the leads,  $\rho_\sigma(\omega) = (2D)^{-1}$  for  $|\omega| < D$  and  $\rho_\sigma(\omega) = 0$  otherwise. Despite the local character of the coupling the spin-spin correlations are not reduced to the two coupled sites, but form some extended object instead. Henceforth, we call it the *Heisenberg cloud* and illustrate it together with relevant phase diagram in Fig. 1(b) and (d). As one can expect from analogy with the Kondo cloud, the normalized spectral density at the coupled sites vanishes in this Heisenberg phase,  $\mathcal{B}(\omega) \sim \omega^2$  for small  $\omega$ . We note that such a mutual screening of different bands may be of importance in some Kondo lattices.

*Heisenberg quasi-particles in direct exchange model.*—The model illustrated in Fig. 1(b) can be seen as a special case of JV model, or even more general PH-symmetric 2-impurity Anderson model, with the Hamiltonian of the latter being

$$H_{\text{direct}} = \sum_{\alpha\mathbf{k}\sigma} \varepsilon_{\alpha\mathbf{k}} c_{\alpha\mathbf{k}\sigma}^\dagger c_{\alpha\mathbf{k}\sigma} + \sum_{\alpha\mathbf{k}\sigma} v_{\alpha\mathbf{k}} (c_{\alpha\mathbf{k}\sigma}^\dagger d_{\alpha\sigma} + \text{H.c.}) - \frac{U}{2} \sum_{\alpha\sigma} n_{\alpha\sigma} + U \sum_{\alpha} n_{\alpha\uparrow} n_{\alpha\downarrow} + J_H \vec{S}_1 \circ \vec{S}_2, \quad (2)$$

where  $v_{\mathbf{k}\sigma}$  denotes the impurity-host hybridization for lead  $\alpha$ ,  $U$  is the Coulomb interaction,  $d_{\alpha\sigma}$  annihilates an electron with spin  $\sigma$  at impurity  $\alpha$ ,  $\vec{S}_\alpha$  is the spin operator there, and  $n_{\alpha\sigma} = d_{\alpha\sigma}^\dagger d_{\alpha\sigma}$ . For the sake of simplicity we assume momentum-independent hybridization terms, identical for both host-impurity pairs, *i.e.*  $v_{\alpha\mathbf{k}} = v$ . Within NRG treatment, the leads are mapped onto semi-infinite tight-binding chains, with one impurity attached at the end of each chain and all chain parameters depending only on the hybridization function  $\Gamma_K(\omega) = \pi\rho(\omega)v^2$ , which for regular functions  $\Gamma_K(\omega)$  can be reduced to its Fermi-energy value  $\Gamma_K$ , if one is interested only in the low-temperature limit [23]. This model is significantly different than in the single-host two-impurity setup, where also two chains appear, but with two different, necessarily energy-dependent and non-PH-symmetric hybridization functions [19]. In the limit  $U \rightarrow 0$ , the Hamiltonian (2) is reduced to  $H_{\text{leads}}$ , Eq. (1), only with  $\Gamma_K$  slightly alternated at large  $\omega$  and  $J_Y$  replaced by  $J_H$ . In this way, RKKY phase in JV model may be seen as a generalization of the Heisenberg phase.

However, for  $U > 0$  the physics changes dramatically, due to emergence of the Kondo scale. To precisely define it, we consider a hypothetical conductance through the impurity,  $G(T) = -\int f_T'(\omega)\mathcal{A}(\omega)d\omega$ , where  $f_T'(\omega)$  is a derivative of the Fermi distribution function. We plot  $G$  in Fig. 2(a) as a function of  $T$ . The single-impurity Kondo scale,  $T_K^0$ , can be defined for  $J_Y = 0$ , as such a temperature that  $G(T_K^0) = G_0/2$ . This is further used as a measure of the strength of the Kondo coupling  $J_K$  stemming from hybridization  $\Gamma_K$ . The figure is prepared for  $U = D/2$  and  $\Gamma_K \approx 0.0492U$  which gives  $T_K^0 \approx 10^{-4}U$ .

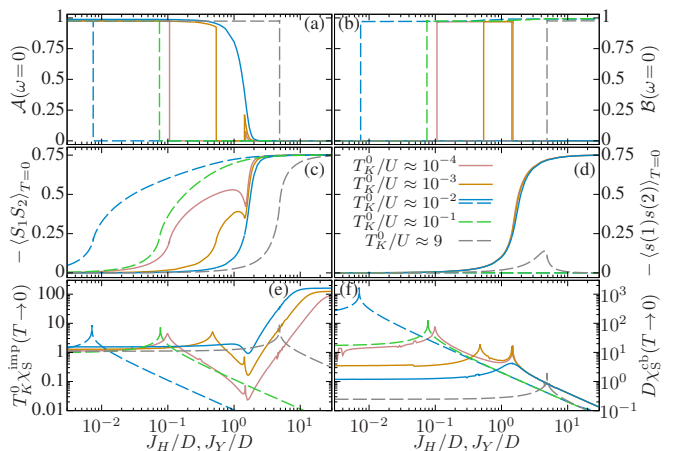


Figure 3. The signatures of the QPTs. Normalized spectral densities (a) at impurity,  $\mathcal{A}$ , and (b) of conduction electrons at the impurity site,  $\mathcal{B}$ , both at 0 energy, as functions of the exchange couplings. Solid (dashed) lines correspond to *genuine (direct)* RKKY exchange model. Panels (c) and (d) show static spin-spin correlations for relevant impurity and conduction band sites, correspondingly, while (e) and (f) present respective staggered susceptibilities.

For  $J_H = 0$  the relevant quasi-particles are Kondo ones, as the two impurity-chain pairs are then completely independent. The direct inter-impurity exchange couples them, and when the coupling exceeds a threshold  $J_H^* \approx 1.5T_K^0$ , the QPT described by Jones and Varma occurs, at which Kondo quasi-particles disintegrate, and the Bloch electrons become relevant (Ref. [6] gives  $J_H^* = 2.2T_K$  for Kondo model instead of Anderson model solved here and slightly different definition of  $T_K^0$ ). JV QPT and the Heisenberg QPT defined earlier share characteristic features, such as  $\mathcal{A}$  and  $\mathcal{B}$  discontinuity [note that now  $\mathcal{A}(0)$  becomes 0 in the *Heisenberg* phase, not  $\mathcal{B}(0)$ , as this is the local spectral density at the sites coupled by the inter-channel exchange interaction],  $\chi_S^{\text{imp}}$  and  $\chi_S^{\text{cb}}$  divergence and smooth dependence of all static spin-spin correlations. These can be seen in dashed lines in Fig. 3.

Moreover, the scale  $T_K^0$  is well defined also in the resonant regime, *i.e.* for impurity-host hybridization  $\Gamma_K \gg U$  or even  $\Gamma_K \gg D$ . The strong charge fluctuations do not destabilize the Kondo fixed point, and the JV QPT is still present in the system at  $J_H^* \sim 1.5T_K^0$ , although the precise transition point is shifted toward larger  $J_H$ , see the phase diagram in Fig. 4(a).

*JV QPT for genuine Y.*—The main purpose of the present study is to analyze how the QPT landscape changes when the spin exchange between the impurities is

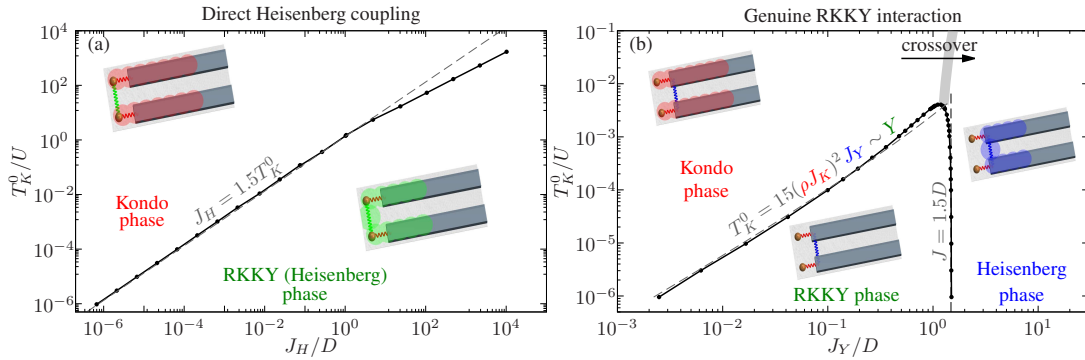


Figure 4. Phase diagrams in different cases. (a) Two-impurity Anderson model with direct inter-impurity exchange. The calculated QPT positions are shown with black points, connected with lines for clarity. (b) Two-impurity Anderson model with genuine RKKY interaction. The insets show the schematics of relevant systems.

genuinely indirect, that is the Hamiltonian has the form

$$H_{\text{genuine}} = \sum_{\alpha\mathbf{k}\sigma} \varepsilon_{\alpha\mathbf{k}} c_{\alpha\mathbf{k}\sigma}^\dagger c_{\alpha\mathbf{k}\sigma} + \sum_{\alpha\mathbf{k}\sigma} v(c_{\alpha\mathbf{k}\sigma}^\dagger d_{\alpha\sigma} + \text{H.c.}) - \frac{U}{2} \sum_{\alpha\sigma} n_{\alpha\sigma} + U \sum_{\alpha} n_{\alpha\uparrow} n_{\alpha\downarrow} + J_Y \vec{s}_1 \circ \vec{s}_2, \quad (3)$$

which differ from Eq. (2) only via the last term, where direct inter-impurity exchange  $J_H$  has been replaced by genuine indirect inter-host coupling  $J_Y$ . Note that the impurities are by assumption attached exactly to the same sites of the host, which are coupled by  $J_Y$ . This is motivated by simplicity and experimental setup [20], where the impurities are formed from  $f$ -electron orbitals of cobalt ad-atoms, while  $s$ -shells of the latter contribute to the hosts conduction band and are exchange-coupled when the two impurities become close to each other. Lifting this assumption would not lead to qualitatively different behavior, which will be shown elsewhere.

The presence of  $J_Y$  leads to genuinely indirect RKKY exchange between the impurities,  $Y = c(\rho J_K)^2 J_Y$ , where  $J_K = 8\Gamma_K/(\pi U)$  is the host-impurity Kondo coupling and  $c$  is a proportionality constant. Let us first discuss weak bare Kondo coupling case, when  $T_K^0 \ll D$ . Then, JV QPT is present at  $Y \approx 1.5T_K^0$  (this actually allows to pinpoint  $c \approx 7.5$ ). The transition can be recognized from discontinuities of  $\mathcal{A}(0)$ , see Fig. 3(a), and  $\mathcal{B}(0)$ , see Fig. 3(b), as well as from the diverging staggered spin susceptibilities  $\chi_S^{\text{imp}}$  and  $\chi_S^{\text{cb}}$ , see Fig. 3(e) and (f), respectively.

*The Kondo breakdown at JV QPT.*—There has been a debate concerning the fate of the Kondo scale near JV QPT, and Kondo destruction at finite  $T_K$  has been predicted on the basis of perturbative renormalization group analysis [21], as an alternative for continuous  $T_K \rightarrow 0$  transition [33]. In Fig. 2(a) we immediately see that for curves corresponding to the Kondo fixed point at  $T = 0$ , in general two different energy scales appear. One is related to departure from local-moment regime, relevant at high  $T$ , and is denoted  $T_W$ . The other is a scale at which

the strong coupling fixed point is actually achieved—we denote it  $T_S$ . In the single-impurity case they are both proportional, but this is no longer the case for two impurities. We present  $T_W(J_Y)$  and  $T_S(J_Y)$  dependencies in Fig. 2(c); the scales are defined by  $G(T_W) = G_0/4$  and  $G(T_S) = 0.9G_0$ .  $T_W$  indeed remains non-zero at QPT, as predicted in Ref. [21]. However, it decreases further in the RKKY phase and vanishes abruptly at some critical  $J_Y$ , when the RG flow is directly from local moment toward RKKY fixed point, without ever reaching  $G = G_0/4$ . At this critical value  $T_W = T_W^0/e$ , *i.e.* the reduction of the weak coupling Kondo scale by factor larger than  $e$  is inconsistent with flow “in direction of” the Kondo fixed point, in agreement with [21]. On the contrary,  $T_S$  becomes arbitrarily small close to the QPT point. All these results remain valid also in JV direct exchange model.

*Heisenberg QPT for genuine  $Y$ .*—In Fig. 3 it is evident, that another QPT occurs at very strong  $J_Y^\ddagger \approx 1.5D$ . This is, in fact, a transition into Heisenberg phase, as in Fig. 1(b) and (d). Actually, for  $\Gamma_K = 0$  the model (3) is equivalent to (1) with 2 additional decoupled impurities. For finite  $\Gamma_K$  impurities hybridize with very first sites of the chains and become parts of a Heisenberg cloud. Then,  $\mathcal{A}(0)$  becomes non-universal [see solid lines in Fig. 3(a)], while  $\mathcal{B}(0)$  is still 0 [Fig. 3(b)]. The divergence of  $\chi_S^{\text{imp}}$  and  $\chi_S^{\text{cb}}$  is still observed as a hallmark of QPT, see Fig. 3(e)-(f). Static spin-spin correlations remain smooth, although  $\langle \vec{S}_1 \circ \vec{S}_2 \rangle_{T=0}$  exhibits a kink around  $J_Y = J_Y^\ddagger$ , as shown in Fig. 3(c-d). It seems noteworthy that the QPT at  $J_Y = J_Y^\ddagger$  resembles the one described in Ref. [34]. However, here the decoupling is not complete, despite the same  $\mathcal{B}(\omega) \sim \omega^2$  in the absence of the impurities. This is due to the fact that the hosts are still correlated via  $J_Y$ , which is not quadratic form of creation and annihilation operators, and the local spectral density is not a complete description of the system. Still, for small  $T_K^0$  the spectral density  $\mathcal{A}(0)$  is very small at the transition and dies out very fast with increasing

$J_Y$  further in the Heisenberg phase.

*Continuous Kondo–Heisenberg crossover.*—Top grasp the complete phase diagram, one has to realize, that while  $J_Y^\ddagger \approx 1.5D$  does not depend on the Kondo coupling,  $J_Y^*$  is proportional to  $T_K^0$ , such that the two critical lines meet at sufficiently strong  $T_K^0$ , as illustrated in Fig. 4(d). Therefore, above the critical value of the Kondo coupling, there is no QPT in the model with *genuine* RKKY coupling, only continuous crossover—even in the most PH-symmetric case. This is illustrated by a solid curves for  $T_K^0/U = 10^{-2}$  in Fig. 3 and means a continuous transformation of the Kondo quasi-particles into Heisenberg ones upon increasing  $J_Y$ . Some signs of it are visible already at slightly lower  $T_K^0$ , where detour form  $\mathcal{A}(0) = 1$  on the Kondo site is seen in Fig. 3 [note  $\mathcal{B}(0) = 0$  in both phases].

*Proposal for experimental realization.*—In conventional materials achieving a spin exchange overwhelming the band-width may seem an impossible task. However, a novel class of Moiré super-lattices, including twisted bilayer graphene, delivers materials with exceptionally flat, isolated conduction bands [35]. This leads to prominent correlation effects [36, 37], and may be utilized for obtaining large spin-exchange to band-width ratios in a geometry of Ref. [20], with two twisted bilayers replacing the golden hosts.

*Summary.*—We have shown that the phase diagram of two impurities on two separate, but spin-exchange-coupled hosts, differs tremendously from the well-known Jones-Varma phase diagram, which mimics the Doniach perspective on the heavy-fermion criticality. We believe that the picture stemming from our analysis, where direct interactions  $J_Y$  and  $J_K$  together induce indirect one RKKY coupling  $Y$ , but generally have competing nature and lead to two QPTs or only a crossover (depending on the strength of  $J_K$ ) may actually be quite a generic scenario, observable in a two-host-two-impurity problem with flat-band materials used as hosts. If analogues exist in heavy-fermion compounds, remains an intriguing question for further study.

The work has been supported by A. von Humboldt Foundation.

---

\* [kpwojcik@ifmpan.poznan.pl](mailto:kpwojcik@ifmpan.poznan.pl)

† [kroha@th.physik.uni-bonn.de](mailto:kroha@th.physik.uni-bonn.de)

- [1] H. v. Löhneysen, A. Rosch, M. Vojta, and P. Wölfle, Fermi-liquid instabilities at magnetic quantum phase transitions, *Rev. Mod. Phys.* **79**, 1015 (2007).
- [2] S. Kirchner, S. Paschen, Q. Chen, S. Wirth, D. Feng, J. D. Thompson, and Q. Si, Colloquium: Heavy-electron quantum criticality and single-particle spectroscopy, *Rev. Mod. Phys.* **92**, 011002 (2020).
- [3] L. Prochaska, X. Li, D. C. MacFarland, A. M. Andrews, M. Bonta, E. F. Bianco, S. Yazdi, W. Schrenk, H. Detz, A. Limbeck, Q. Si, E. Ringe, G. Strasser, J. Kono, and S. Paschen, Singular charge fluctuations at a magnetic quantum critical point, *Science* **367**, 285 (2020).
- [4] S. Paschen and Q. Si, Quantum phases driven by strong correlations, *Nat. Rev. Phys.* **3**, 9 (2021).
- [5] B. A. Jones and C. M. Varma, Study of two magnetic impurities in a Fermi gas, *Phys. Rev. Lett.* **58**, 843 (1987).
- [6] B. A. Jones, C. M. Varma, and J. W. Wilkins, Low-Temperature Properties of the Two-Impurity Kondo Hamiltonian, *Phys. Rev. Lett.* **61**, 125 (1988).
- [7] B. A. Jones and C. M. Varma, Critical point in the solution of the two magnetic impurity problem, *Phys. Rev. B* **40**, 324 (1989).
- [8] A. C. Hewson, *The Kondo problem to heavy fermions* (Cambridge University Press, Cambridge, 1997).
- [9] S. Doniach, The Kondo lattice and weak antiferromagnetism, *Physica B+C* **91**, 231 (1977).
- [10] M. A. Ruderman and C. Kittel, Indirect Exchange Coupling of Nuclear Magnetic Moments by Conduction Electrons, *Phys. Rev.* **96**, 99 (1954).
- [11] T. Kasuya, A Theory of Metallic Ferro- and Antiferromagnetism on Zener’s Model, *Prog. Theor. Phys.* **16**, 45 (1956).
- [12] K. Yosida, Magnetic Properties of Cu-Mn Alloys, *Phys. Rev.* **106**, 893 (1957).
- [13] P. Nozières, Impuretés magnétiques et effet Kondo, *Ann. Phys. Fr.* **10**, 19 (1985).
- [14] F. Eickhoff and F. B. Anders, Strongly correlated multi-impurity models: The crossover from a single-impurity problem to lattice models, *Phys. Rev. B* **102**, 205132 (2020).
- [15] F. Eickhoff and F. B. Anders, Kondo holes in strongly correlated impurity arrays: RKKY driven Kondo screening and hole-hole interactions, *arXiv* (2021), 2104.03626.
- [16] R. M. Fye, Anomalous fixed point behavior” of two Kondo impurities: A reexamination, *Phys. Rev. Lett.* **72**, 916 (1994).
- [17] I. Affleck, A. W. W. Ludwig, and B. A. Jones, Conformal-field-theory approach to the two-impurity Kondo problem: Comparison with numerical renormalization-group results, *Phys. Rev. B* **52**, 9528 (1995).
- [18] R.-Q. He, J. Dai, and Z.-Y. Lu, Natural orbitals renormalization group approach to the two-impurity Kondo critical point, *Phys. Rev. B* **91**, 155140 (2015).
- [19] F. Eickhoff, B. Lechtenberg, and F. B. Anders, Effective low-energy description of the two-impurity Anderson model: RKKY interaction and quantum criticality, *Phys. Rev. B* **98**, 115103 (2018).
- [20] J. Bork, Y.-h. Zhang, L. Diekhöner, L. Borda, P. Simon, J. Kroha, P. Wahl, and K. Kern, A tunable two-impurity Kondo system in an atomic point contact, *Nat. Phys.* **7**, 901 (2011).
- [21] A. Nejadi, K. Ballmann, and J. Kroha, Kondo Destruction in RKKY-Coupled Kondo Lattice and Multi-Impurity Systems, *Phys. Rev. Lett.* **118**, 117204 (2017).
- [22] K. G. Wilson, The renormalization group: Critical phenomena and the Kondo problem, *Rev. Mod. Phys.* **47**, 773 (1975).
- [23] R. Bulla, T. A. Costi, and T. Pruschke, Numerical renormalization group method for quantum impurity systems, *Rev. Mod. Phys.* **80**, 395 (2008).
- [24] O. Legeza, C. P. Moca, A. I. Toth, I. Weymann, and G. Zarand, Manual for the Flexible DM-NRG code, *arXiv:0809.3143* (2008). The code is available at <http://>

[//www.phy.bme.hu/~dmnrg/](http://www.phy.bme.hu/~dmnrg/).

- [25] J. Kondo, Resistance Minimum in Dilute Magnetic Alloys, *Prog. Theor. Phys.* **32**, 37 (1964).
- [26] P. Simon and I. Affleck, Finite-Size Effects in Conductance Measurements on Quantum Dots, *Phys. Rev. Lett.* **89**, 206602 (2002).
- [27] L. Borda, Kondo screening cloud in a one-dimensional wire: Numerical renormalization group study, *Phys. Rev. B* **75**, 041307 (2007).
- [28] H. Prüser, M. Wenderoth, P. E. Dargel, A. Weismann, R. Peters, T. Pruschke, and R. G. Ulbrich, Long-range Kondo signature of a single magnetic impurity, *Nat. Phys.* **7**, 203 (2011).
- [29] I. V. Borzenets, J. Shim, J. C. H. Chen, A. Ludwig, A. D. Wieck, S. Tarucha, H.-S. Sim, and M. Yamamoto, Observation of the Kondo screening cloud, *Nature* **579**, 210 (2020).
- [30] A. Weichselbaum and J. von Delft, Sum-Rule Conserving Spectral Functions from the Numerical Renormalization Group, *Phys. Rev. Lett.* **99**, 076402 (2007).
- [31] F. B. Anders and A. Schiller, Real-Time Dynamics in Quantum-Impurity Systems: A Time-Dependent Numerical Renormalization-Group Approach, *Phys. Rev. Lett.* **95**, 196801 (2005).
- [32] I. Weymann and J. Barnaś, Spin thermoelectric effects in Kondo quantum dots coupled to ferromagnetic leads, *Phys. Rev. B* **88**, 085313 (2013).
- [33] P. Coleman, C. Pépin, Q. Si, and R. Ramazashvili, How do Fermi, *J. Phys.: Condens. Matter* **13**, R723 (2001).
- [34] T. Esat, B. Lechtenberg, T. Deilmann, C. Wagner, P. Krüger, R. Temirov, M. Rohlfing, F. B. Anders, and F. S. Tautz, A chemically driven quantum phase transition in a two-molecule Kondo system, *Nat. Phys.* **12**, 867 (2016).
- [35] R. Bistritzer and A. H. MacDonald, Moiré bands in twisted double-layer graphene, *Proc. Natl. Acad. Sci. U.S.A.* **108**, 12233 (2011).
- [36] Y. Cao, V. Fatemi, A. Demir, S. Fang, S. L. Tomarken, J. Y. Luo, J. D. Sanchez-Yamagishi, K. Watanabe, T. Taniguchi, E. Kaxiras, R. C. Ashoori, and P. Jarillo-Herrero, Correlated insulator behaviour at half-filling in magic-angle graphene superlattices, *Nature* **556**, 80 (2018).
- [37] Y. Cao, V. Fatemi, S. Fang, K. Watanabe, T. Taniguchi, E. Kaxiras, and P. Jarillo-Herrero, Unconventional superconductivity in magic-angle graphene superlattices, *Nature* **556**, 43 (2018).